

High pressure phase diagrams of CeRhIn₅ and CeCoIn₅ studied by ac calorimetry

G Knebel[†], M-A Méasson[†], B Salce[†], D Aoki[†], D Braithwaite[†], J P Brison[‡] and J Flouquet^{†§}

[†] Département de Recherche Fondamentale sur la Matière Condensée, SPSMS, CEA Grenoble, 38054 Grenoble Cedex 9, France

[‡] Centre de Recherche sur les Très Basses Températures, CNRS, 38042 Grenoble Cedex 9, France

[§] Institut de Physique de la Matière Condensée de Grenoble, 38042 Grenoble Cedex 9, France

Abstract. The pressure-temperature phase diagrams of the heavy fermion antiferromagnet CeRhIn₅ and the heavy fermion superconductor CeCoIn₅ have been studied under hydrostatic pressure by ac calorimetry and ac susceptibility measurements using diamond anvil cells with argon as pressure medium. In CeRhIn₅, the use of a highly hydrostatic pressure transmitting medium allows for a clean simultaneous determination by a bulk probe of the antiferromagnetic and superconducting transitions. We compare our new phase diagram with the previous ones, discuss the nature (first or second order) of the various lines, and the coexistence of antiferromagnetic order and superconductivity. The link between the collaps of the superconducting heat anomaly and the broadening of the antiferromagnetic transition points to an inhomogeneous appearance of superconductivity below $P_c \approx 1.95$ GPa. Homogeneous bulk superconductivity is only observed above this critical pressure. We present a detailed analysis of the influence of pressure inhomogeneities on the specific heat anomalies which emphasizes that the observed broadening of the transitions near P_c is connected with the first order transition. For CeCoIn₅ we show that the large specific heat anomaly observed at T_c at ambient pressure is suppressed linearly at least up to 3 GPa.

PACS numbers: 71.27.+a, 74.70.Tx, 74.62.Fj

Submitted to: *J. Phys.: Condens. Matter*

E-mail: gknebel@cea.fr

1. Introduction

Heavy fermion systems provide the unique opportunity to study of the interplay of long range magnetic order, unconventional superconductivity (SC) and valence fluctuations. For usual superconductors the attractive interaction between two electrons forming a Cooper pair is due to a lattice instability and magnetic impurities act as pair breaking. The finding of superconductivity at the verge of an antiferromagnetic ordered state in cerium heavy fermion systems like $CeCu_2Si_2$ [1], $CeCu_2Ge_2$ [2], $CeRh_2Si_2$ [3] $CePd_2Si_2$ and $CeIn_3$ [4] suggested a pairing mechanism associated with the magnetic instability. The importance of critical valence fluctuations for the appearance of SC in systems with strong electronic correlations has been pointed out recently [5, 6].

The discovery of superconductivity in $CeMIn_5$ ($M=Co, Rh, Ir$) compounds opened new routes to investigate the appearance of pressure induced SC in heavy fermion compounds and its interplay with antiferromagnetism (AFM) [7, 8, 9]. While $CeCoIn_5$ and $CeIrIn_5$ are superconductors at ambient pressure with superconducting transition temperatures $T_c = 2.3$ K and 0.4 K, $CeRhIn_5$ is antiferromagnetically ordered below the Néel temperature $T_N = 3.8$ K and SC appears only under hydrostatic pressure. The family of $CeMIn_5$ is closely related to $CeIn_3$ and the crystal structure consists of alternating layers of $CeIn_3$ and MIn_2 stacking along the [001] direction. $CeIn_3$ is due to its cubic structure a nice model system to study the appearance of superconductivity at a quantum critical point where the magnetic order is suppressed, however SC appears only below 0.2 K in the pressure range of 2-3 GPa and the interplay between AFM and SC is experimentally difficult to investigate [4, 10]. The superconducting transition temperatures in $CeCoIn_5$ and $CeRhIn_5$ are enhanced by a factor of almost 10 in comparison to $CeIn_3$. For superconductivity mediated by spin-fluctuations the higher T_c is expected for systems with lower dimensionality [11, 12, 13] and indeed, in the 115 family the Fermi surface is almost two dimensional [14].

The pressure-temperature phase diagram of $CeRhIn_5$ has already been studied by resistivity ρ [15], specific heat C [16], magnetic susceptibility χ , nuclear quadrupole resonance (NQR) [17, 18, 19, 20, 21], and neutron scattering experiments [22, 23, 24, 25]. $CeRhIn_5$ orders at ambient pressure in an incommensurate antiferromagnetic helical structure with a wave vector $\mathbf{q} = (0.5, 0.5, 0.297)$ and a staggered moment of about $0.8 \mu_B$. Contrary to the first measurements [24], recent neutron scattering measurements show no significant change of the magnetic structure and the magnetic moment up to 1.7 GPa [25]. However, a NQR study shows that the internal magnetic field decreases linearly with pressure and approaches slowly a value of about 5% at ambient pressure at 1.75 GPa [18, 19, 20]. The difference between neutron and NQR experiment is generally considered to be due to the different time scale of the measurements. From all measurements, except the very first by Hegger *et al.*, it follows that the antiferromagnetic order is suppressed near 2 GPa. Only the specific heat experiments [16] found some anomaly above T_c at 2.1 GPa: nevertheless, AFM order was discarded as a possible origin for that anomaly [16]. SC has been found with transport measurements in the

pressure range from 1-8 GPa, with the maximum transition temperature $T_c \approx 2.2$ K at $P \approx 2.5$ GPa [15]. For pressures $P > 2$ GPa $CeRhIn_5$ would be an unconventional superconductor with line nodes in the gap as shown by measurements of the NQR relaxation rate $1/T_1$ which has a T^3 dependence below T_c [17, 18], in agreement with specific heat measurements [16]. In the intermediate pressure region between 1.6 and 2 GPa, AFM and SC have been claimed to coexist, with possible "extended gapless" regions in the superconducting gap function. Recent NQR measurements claim to confirm this possibility of gapless superconductivity in the coexistence regime from the observation of a constant $T_1 T$ below $T_c/2$, ascribed to a finite quasiparticle density of states [21].

$CeCoIn_5$ is a unconventional SC with most probably d wave symmetry and line nodes in the gap [17, 26, 27, 28, 29]. At ambient pressure, it is located close to an antiferromagnetic quantum-critical point (QCP). Detailed resistivity measurements show that applying hydrostatic pressure tunes the system away from the proximity of the QCP [30, 31]. The huge anomaly observed in specific heat at T_c at ambient pressure ($\Delta C/C(T_c) = 4.7$) decreases under pressure up to 1.5 GPa [32]. De Haas-van Alphen measurements show cyclotron masses at ambient pressure which are strongly field dependent and decreasing under pressure [33].

In this article we report on detailed ac calorimetric measurements of $CeRhIn_5$ and $CeCoIn_5$ in an extended pressure range up to 3.5 GPa. The measurements were performed in argon loaded diamond anvil cells ensuring almost perfect hydrostatic pressure conditions. The main focus will be on the appearance of SC in the coexistence phase of AFM and SC in $CeRhIn_5$. As the physical properties of the 115 family are very sensitive to uniaxial pressure and pressure inhomogeneities [34] hydrostaticity of the sample environment is very important. Previous specific heat measurements on $CeRhIn_5$ were performed in piston cylinder type cell with a solid pressure transmitting medium (AgCl) [16]. Even if the pressure difference between different ends of the sample is quite small, the effect of stress on the sample is not negligible. The nature of the superconducting transition in $CeRhIn_5$ at high pressure will be related to that of $CeCoIn_5$. The main result is for $CeRhIn_5$ the observation of nice specific heat anomalies at the antiferromagnetic transition at low pressure and at the superconducting transition above 2 GPa. Superconductivity appears in specific heat measurements only very close to the critical pressure where both transitions are tiny and rather broad. From the pressure dependence of the superconducting anomaly $\Delta C/C(T_c)$ it follows that in $CeCoIn_5$ at ambient pressure, SC sets in when the effective mass of the electrons is still increasing towards low temperatures due to the formation of the heavy fermion state, whereas at 3 GPa it behaves like a usual heavy fermion superconductor. For both compounds the effect of pressure inhomogeneities on the magnetic and superconducting transition will be discussed.

As regard notations, we call P_{S-} the lowest pressure for which superconductivity is observed, P_{S+} the highest pressure for which superconductivity is observed, and P_c , the pressure of the point where the AFM transition line $T_N(p)$ meets the superconducting

transition line $T_c(P)$. Let us remind here that the antiferromagnetic state is also labelled "AFM", the superconducting state "SC", a coexisting AFM and SC state "AFM+SC", and the paramagnetic state "PM".

2. Experimental details

High quality single crystals of $CeRhIn_5$ and $CeCoIn_5$ have been grown by the In flux method [7]. The specific heat measurements under pressure were performed using ac calorimetry. In the case of $CeRhIn_5$ we set up two pressure cells giving almost identical results. Details of this technique for measurements of the specific heat are given elsewhere [35, 36, 37]. The samples studied were of size of about $200 \times 200 \times 60 \mu m$. An AuFe/Au thermocouple served to measure the temperature oscillations of the sample. It is soldered directly on the sample to ensure a good thermal contact between thermometer and sample. As heater we used a 50 mW argon laser. By using a mechanical chopper it is possible to obtain a quasi sinusoidal power which is transmitted by optical fibre directly to the sample. However, this method doesn't allow quantitative measurements, as the heating power is not focused on the sample, but irradiates also the pressure transmitting medium (argon) and the gasket which are heated and contribute to an additional background signal which changes between different experiments. To find the optimal working frequency ν , the frequency dependence of the ac signal was measured at 1.5 K and 4.2 K. The cut off frequency ν_c was found to be about 600 Hz, the measurements were performed at 831 Hz slightly above ν_c . The specific heat of the sample can be estimated by $C_{ac} \propto -PS_{th} \sin(\theta - \theta_0)/V_{th}2\pi\nu$ where V_{th} and S_{th} are respectively the measured voltage and the thermopower of the thermocouple. As the origin of the phase θ_0 cannot be determined by our method, we neglect in the analysis the contribution of the phase signal. However a comparison of the behaviour of the signal at low pressure with an absolute measurement at ambient pressure shows, that observed ac signal is correct.

The ac susceptibility was measured in an argon loaded sapphire anvil cell with 2.5 mm tables diameter. Both anvils are placed inside one of the detection coils (5000 turns), the second detection coil is placed above the anvils. In this geometry the sample and the gasket are in the middle of the lower detection coil. This geometry allows a very good compensation of the susceptometer at fixed temperature, however the filling factor is poor. An additional difficulty is coming from a temperature drift of the background signal which cannot be compensated. The measurements were performed at 71 Hz, and before each run the susceptometer was offset at the lowest temperature by compensating the amplitude and the phase of the signal with a small compensation coil which is wounded directly on the excitation coil. This susceptometer allows the detection of the onset temperature of the superconducting transition due to the diamagnetic shielding, however it is not possible to conclude about the superconducting volume fraction. The total volume of the measured samples was about 0.01 mm^3 .

In both experiments the pressure was determined in-situ at low temperatures by

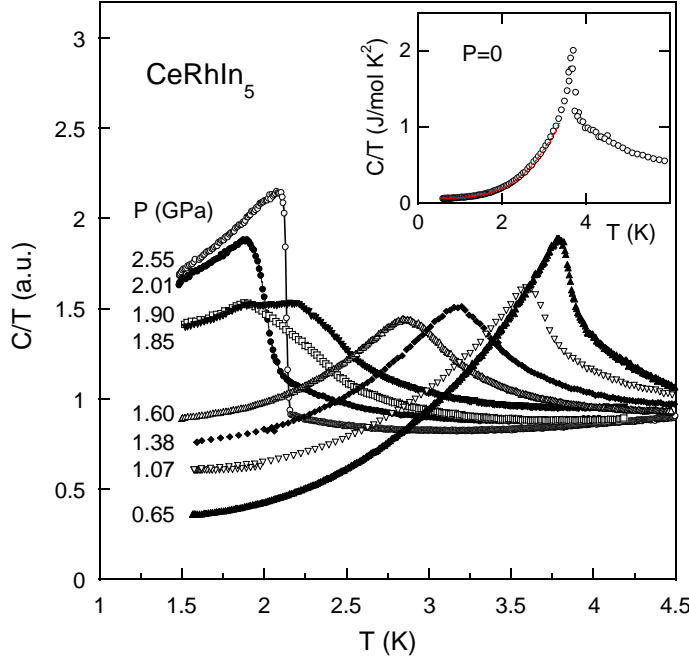


Figure 1. Specific heat of CeRhIn_5 for different pressures p (pressure cell #1). The data are normalized at $T = 5$ K. The inset shows the specific heat measured at ambient pressure.

the ruby fluorescence at 4.2 K. A bellows system allows to change and fine tune the pressure at low temperature [38].

3. Specific heat of CeRhIn_5 under pressure

3.1. Experimental results

The temperature dependence of the specific heat signal of CeRhIn_5 is plotted in figure 1 for different pressures. The inset shows the specific heat of CeRhIn_5 at ambient pressure. At T_N , C/T has a very sharp peak at ambient pressure. The entropy connected with the magnetic transition is small, of about $0.3R \ln 2$. The remaining entropy is recovered up to 20 K. This strong enhancement of the specific heat in the vicinity of T_N shows the importance of short range order (magnetic fluctuations) and is not described by mean field theory. In the magnetically ordered state, C/T can be best approximated by taking into account an electronic contribution $C_{el}/T = \gamma + \beta_M T^2$ and an additional term corresponding to an antiferromagnetic spin wave with a gap in the excitation spectrum $C_g/T = \beta'_M e^{-\Delta/T}$ [39]. As parameter we find $\gamma = 52 \text{ mJ/mol K}^2$, $\beta_M = 24 \text{ mJ/mol K}^4$, $\beta'_M = 756 \text{ mJ/mol K}^4$, and $\Delta = 8.1 \text{ K}$. In comparison to the anomaly at T_N at ambient pressure, at 0.6 GPa the magnetic anomaly is shifted to higher temperatures and the transition is only slightly broadened. The magnetic ordering temperature T_N is determined by the maximum of C/T . With increasing pressure above 0.6 GPa, T_N is decreasing and for pressures higher than 1 GPa the transition

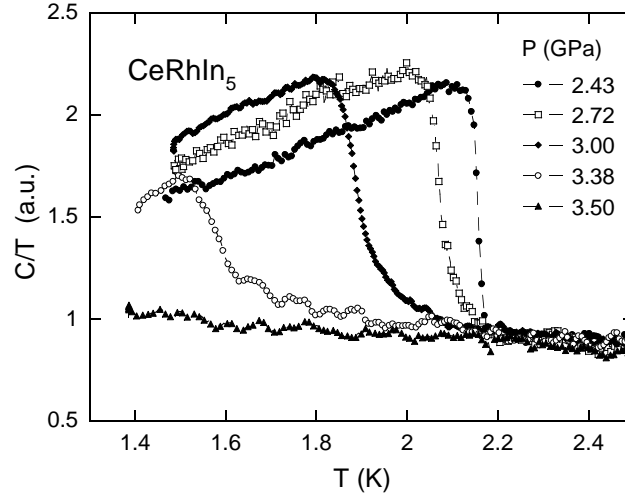


Figure 2. Superconducting transition at high pressures for $CeRhIn_5$ (pressure cell #2). C/T is normalized in the normal state at $T = 2.2$ K.

starts to broaden, however the magnetic anomaly remains well defined. At 1.85 GPa the magnetic anomaly at $T_N = 2.2$ K is very broad. A second maximum associated with a superconducting transition is observed at lower temperatures at $T_c = 1.8$ K. Increasing the pressure by only 0.05 GPa leads to a suppression of the maximum at the magnetic transition, and only a shoulder above T_c points to an antiferromagnetic state. With further increasing pressure, the superconducting transition gets more pronounced and at 2 GPa, slightly above $P_c = 1.95$ GPa, only a clear superconducting transition is found. In the investigated temperature range $T > 1.4$ K we see no sign of a magnetic transition above P_c in the superconducting phase. The superconducting transition increases up to 2.21 K at 2.4 GPa. Increasing further the pressure leads to a suppression of T_c (see figure 2).

In figure 3 the ac susceptibility signal connected with the superconducting transition is plotted. A superconducting anomaly is first seen at 1.5 GPa, but the width of the transition $\Delta T_c = 200$ mK is very large. With increasing pressure the transition width gets smaller and T_c is increasing ($\Delta T_c = 50$ mK at 2.3 GPa) where the maximum $T_c = 2.21$ K is observed. For $P < P_c$ and for $P > 2.5$ GPa the onset of the superconducting transition by susceptibility (T_c^x) is at higher temperatures than the onset of the transition by specific heat (T_c^C). A cascade $T_c^p > T_c^x > T_c^C$ of superconducting transition temperatures determined by resistivity (T_c^p), susceptibility and specific heat measurements is characteristic of heterogeneous material.

3.2. Phase diagram of $CeRhIn_5$

In figure 4, we summarize the phase diagram of $CeRhIn_5$ obtained by specific heat and susceptibility measurements. In addition we plotted T_c obtained by resistivity measurements (+) from Llobet *et al.* [25]. The phase diagram of $CeRhIn_5$ can be

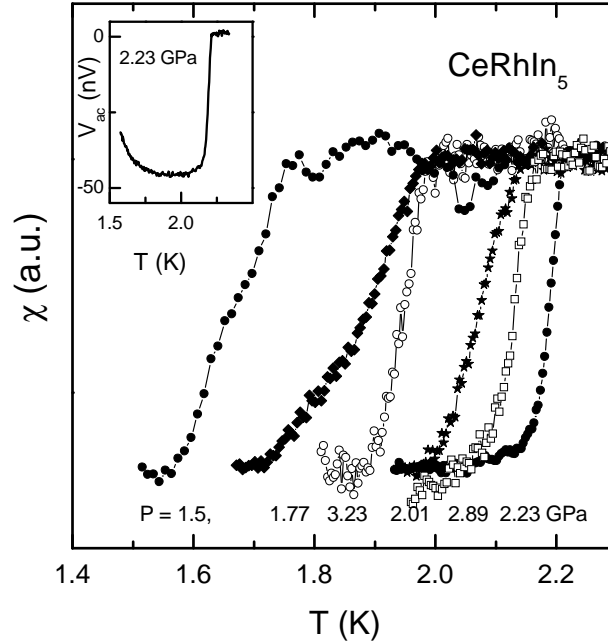


Figure 3. Superconducting transition of CeRhIn_5 observed in ac susceptibility. The amplitude of the transition is arbitrary and scaled for different pressures. The onset of the transition is very sharp only above the critical pressure $P_c = 1.9$ kbar. The inset shows the observed signal in absolute units for 2.23 GPa. The increase of the signal to low temperatures is due to the background.

divided in three different parts: at low pressure, $P < 0.9$ GPa, the ground state is purely antiferromagnetic. In a limited pressure range $0.9 \text{ GPa} < P < 1.95$ GPa superconductivity and antiferromagnetism may coexist, and for $P > 1.95$ GPa the ground state is superconducting. The AFM transition line $T_N(P)$ meets the SC transition line at $P_c \approx 1.95$ GPa.

Let us first discuss the AFM transition. At low pressures $T_N(P)$ is first increasing with pressure and has a smooth maximum at $P \approx 0.6$ GPa. In the intermediate pressure range $0.9 \text{ GPa} < P < 2$ GPa, T_N is monotonously decreasing up to 1.9 GPa, with a continuously increasing rate exceeding 2 K/GPa at P_c . Near P_c , the magnetic transition gets very broad and the amplitude of the magnetic transition is strongly decreasing compared to the low pressure measurements. These broadening effects will be more quantitatively discussed in the next section. Let us note that both NQR and specific heat measurements agree on the fact that above P_c , no AFM order is observed : the ground state for $P > P_c$ is a pure superconducting state. As regard even the latest neutron measurements [25], they do not extend beyond 1.85 GPa. However, the strange result (in apparent contradiction with the slow NQR probe (10^{-7} s)) is that the low temperature ordered moment determined by a quasi-instant probe as neutron scattering (10^{-11} s) does not collapse with T_N close to P_c , but the staggered moment is almost constant up to 1.85 GPa.

Switching now to the superconducting transition, the most remarkable fact is the

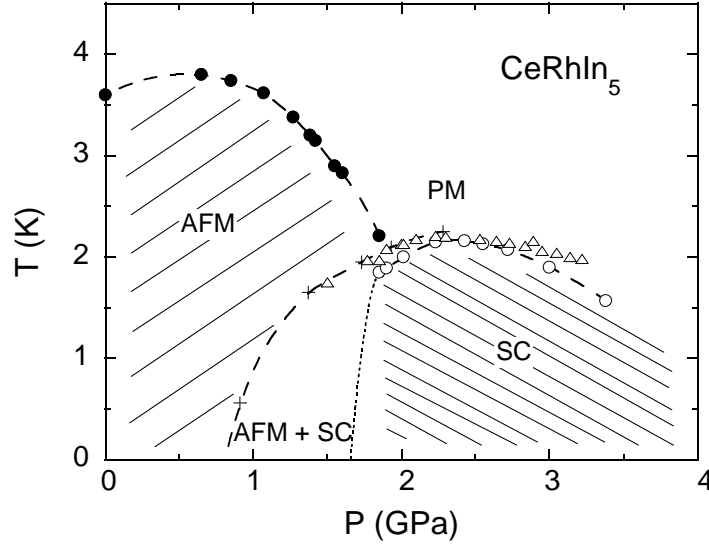


Figure 4. Phase diagram of CeRhIn_5 as determined by specific heat (\bullet and \circ) and susceptibility measurements (\triangle). In addition $T_c(p)$ from resistivity measurements ($\rho = 0$) after Llobet *et al.*[25] is plotted ($+$). The hatched areas mark the regimes where pure AFM and pure SC states are observed. The dotted line indicates the most probable first order line between the AFM and the SC bulk phase; in the (AFM+SC) regime SC is expected to be only filamentary and not a bulk property.

absence of AFM order below T_c above P_c : for $P > P_c$ the ground state is a pure superconducting state. Nice superconducting anomalies are observed, becoming sharper near the maximum $T_c = 2.2$ K at 2.55 GPa. At this pressure, the transition width is comparable to the superconducting transition in CeCoIn_5 at ambient pressure. For higher pressures T_c determined from the specific heat experiment decreases with a rate of -0.7K/GPa . Resistivity measurements by Muramatsu *et al.* show that superconductivity is completely suppressed at a pressure P_{S+} of ≈ 8 GPa [15]. Contrary to the previous work [16], we do not observe any round anomaly above P_c due to its normale phase, and a fortiori no sign of AFM transition. In agreement with [16], we also do not observe any sign of an AFM transition below T_c , even very close from P_c . So in CeRhIn_5 , T_N is not suppressed continuously to zero, but has a finite value at P_c . It demonstrates the absence of a quantum critical point in CeRhIn_5 . Thermodynamically, it means that once T_c is above T_N , the free energy of the superconducting state is lower than that of the AFM state, whatever the temperature, and that in CeRhIn_5 , contrary to the usual consensus on heavy fermion superconductors, AFM order and superconductivity compete.

This has also consequences on the pairing mechanism: this competition and the closeness of the energy scales of both phenomenon, makes the AFM correlations as a sole source of the pairing mechanism very unlikely. For example, an extraordinary strong coupling regime would be required to explain that the maximum T_c is so close (a factor of ≈ 2) to the maximum T_N . Further, the superconducting anomaly $\Delta C/C(T_c)$

is largest in the pressure range from 2.5 GPa to 3 GPa, pointing to the maximum of the pairing interaction for SC above P_c . Interestingly this is the pressure range where the resistivity has a linear temperature dependence above T_c and the residual resistivity ρ_0 a maximum as function of pressure [15]. This points to the probable importance of valence fluctuations in the superconducting pairing mechanism [5].

The regime above P_c puts also severe constraints on the possible coexistence regime below P_c . In resistivity measurements on high quality crystals in Los Alamos[25], SC is found down to much lower pressures than P_c : $P_{S-} \approx 0.9$ GPa. The extrapolation of $T_c \rightarrow 0$ coincides almost with the pressure of the maximum of T_N . The transition temperatures T_c determined from the ac susceptibility measurements are in good agreement with these resistivity measurements. However, with ac calorimetry, we find a superconducting anomaly only very close to the critical pressure $P_c = 1.95$ GPa. This questions the homogenous coexistence of superconductivity and antiferromagnetism in this pressure range, as the observed transitions in resistivity and susceptibility are not a bulk probe of superconductivity. From the specific heat measurements, we know that at 1.5 GPa, T_c , if non zero, is below 1.5 K. So instead of $P_{S-} \approx 0.9$ GPa, we expect an almost vertical line between P_{S-} and P_c . This would mean that the line $T_c(P)$ drawn by resistivity or susceptibility measurements within the AFM state does not reflect a bulk transition, and might be connected to internal stress inside the sample, like in $CeIrIn_5$ [40]. This also means that previous claims of a coexistence of AFM order and superconductivity [25, 21] relying on the observation of AFM order below the resistive T_c in the pressure range between P_{S-} and P_c are not a definite proof of that coexistence. Differences in T_c^x and T_c^C are also observed above 2.5 GPa, the pressure of maximum T_c . Of course, in our scenario of a direct AFM \rightarrow SC transition, the line between AFM and SC is expected to be a first order line, owing to the sudden disappearance of the magnetic order parameter (and in agreement with the strong slope of $|\frac{\partial T_c}{\partial P}|$). Further intrinsic phase separation with a mixed phase may be possible. In $CeIn_3$, phase separation was nicely demonstrated by NQR [41].

To summarize this discussion, from our specific heat and ac susceptibility measurements, two different scenarii are possible; (i) the appearance of superconductivity in the antiferromagnetic ordered state is not homogenous and no true AFM+SC state exists. The experimental observations would then result from superconducting filaments, which can be created due to internal stress induced by dislocations or stacking faults, or due to a phase segregation in a pure magnetically ordered and in a superconducting volume fraction. With increasing pressure the antiferromagnetic volume is decreasing and the paramagnetic volume which has a superconducting ground state increases. Above P_c , only the superconducting state survives. (ii) The coexistence is really homogenous, which means that the same electrons are responsible for the antiferromagnetic order and for superconductivity. In this case the missing anomaly of specific heat is due to a gapless superconducting state which is not explained by impurities, and the coexistence phase corresponds to a new class of superconducting states [42]. In the following, both possibilities will be discussed, also we strongly believe in the first scenario.

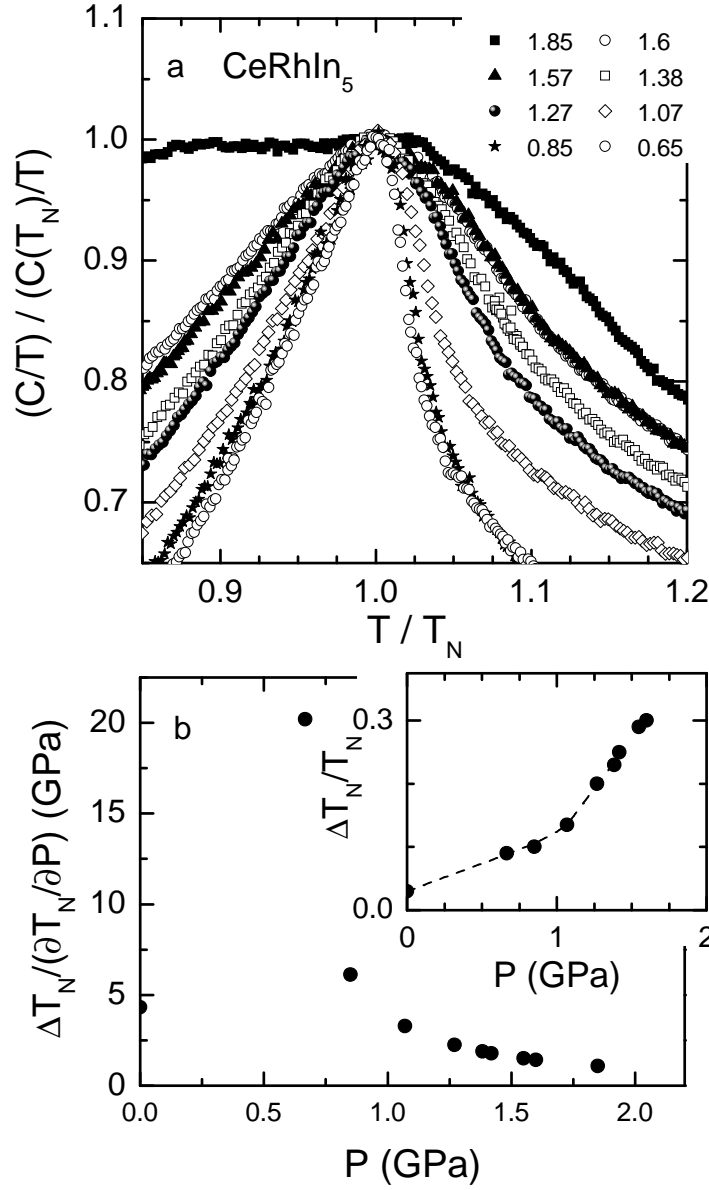


Figure 5. Upper frame a) Specific heat anomaly due to the antiferromagnetic order of CeRhIn_5 normalized by the maximum of C/T at T_N as function of T/T_N . Lower frame b) the transition width ΔT_N normalized by the slope of the variation of T_N versus p . The width of the transition is arbitrarily taken at $(C(T)/T)/(C(T_N)/T) = 0.8$. The inset shows the relative width of the antiferromagnetic transition $\Delta T_N/T_N$ observed in the specific heat experiment as function of pressure.

3.3. On the transition broadening

Figure 5a shows the specific heat in a normalized representation $\frac{C(T)/T}{C(T_N)/T}$ as function of T/T_N . To quantify the observed broadening of the magnetic anomaly, we arbitrarily define the full width of the transition when $\frac{C(T)/T}{C(T_N)/T} = 0.8$. The relative width of the antiferromagnetic transition as a function of pressure is then shown in the inset of figure 5b. A change of regime is clearly visible at 0.9 GPa where T_N starts to decrease and

superconductivity is observed by Llobet et al.[25]. At low pressure the anomaly is rather sharp, but for $P > 0.9$ GPa it gets continuously broader. However, several effects come into play. Part of the width is intrinsic, coming from the fluctuations, and it is expected to yield a constant value of $\frac{\Delta T_N}{T_N}$. In addition, material inhomogeneities, internal or external stress, pressure gradients, might give a pressure dependent contribution to $\left(\frac{\Delta T_N}{T_N}\right)$. Some of these effects will be proportional to the pressure variation of T_N and so to $\frac{\partial T_N}{\partial P}$ in a first approximation (see 5b). Detailed measurements show that the pressure variation in a diamond anvil cell with argon in the low pressure range ($P < 6$ GPa) is generally lower than 0.04 GPa [43]. Considering the width and also the shape of the ruby spectra, we could not detect any significant broadening of these spectra over the whole investigated pressure range. If the observed broadening would result only from pressure inhomogeneities in the pressure cell, this would require pressure inhomogeneities of the order of 0.055 GPa near $P_c = 1.95$ GPa, which can be excluded.

Further, the observed very sharp superconducting transition at 2.4 and 2.55 GPa in different pressure cells are a posteriori a strong indication of high hydrostaticity. Here the width of the transition, $\Delta T_c = 3$ mK, is comparable to the superconducting transition of $CeCoIn_5$ at ambient pressure (see below). This clearly shows that the broadening of the magnetic transition on approaching the critical point is not related to the pressure cell. Similar behaviour has been observed in other heavy fermion systems like $CeIn_3$ [10], $CePd_2Si_2$ [44] and $CeRh_2Si_2$ [45] too. Theoretically, in the case of a second order phase transition which ends at the critical pressure P_c , the form of the mean field magnetic transition for $T_N \rightarrow 0$ is sharp. Only the size of the anomaly is decreasing as the ordered magnetic moment is decreasing [46], which is not even the case in $CeRhIn_5$ [25]. As regard impurity effects, in the classical framework of a second order phase transition (Harris criterion [47]), they are believed to change the critical behaviour only if the specific heat diverges at T_N .

Here the phenomena is quite different and more similar to surface problems found in magnetism or for some local structural transitions. Physically it seems that the magnetic coherence length at T_N cannot exceed a critical value ξ_c . As for $P \rightarrow P_c$ the magnetic coherence length at $T \rightarrow 0$ will increase strongly, there is a severe cut off in the development of a large coherence length and thus in a corresponding smearing of the specific heat anomaly.

In the pressure range of a first order transition the entropy drop ΔS associated to the magnetic transition is linked to the slope of $\partial T / \partial P$ according to the Clapeyron relation $\partial T / \partial P = \Delta V / \Delta S$, where ΔV is the volume discontinuity. The final vertical slope of $\partial T / \partial P$ as $T \rightarrow 0$ reflects the collapse of the entropy in agreement with the Nernst principle. As the material is highly sensitive to imperfections, the entropy drop corresponds to a broad specific heat anomaly. The corresponding entropy contribution ΔS reflects the amplitude of $\partial T / \partial P$ as by contrast the volume discontinuity may change weakly under pressure. So it is quite reasonable that the specific heat anomaly of the magnetic transition disappears drastically on approaching P_c .

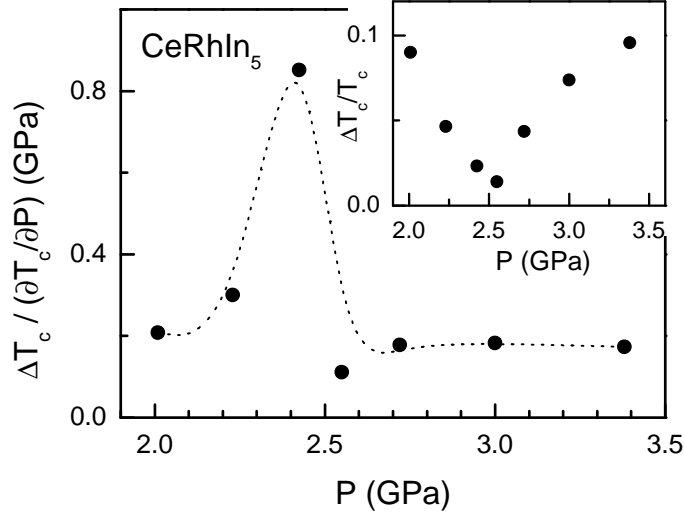


Figure 6. Width of the superconducting transition in CeRhIn_5 in the ac calorimetry normalized by the slope of T_c versus P . It is basically constant, the high point at P_c coming from the residual finite width divided by a vanishing $\frac{\partial T_c}{\partial P}$. Inset: Relative width of the superconducting transition from specific heat experiments in CeRhIn_5 as function of pressure.

Internal stress may lead to drastic features as antagonistic behavior are often observed in the variation of the Néel temperature for a strain σ applied in nonequivalent directions. Well known examples for tetragonal systems are CePd_2Si_2 [48, 49] or URu_2Si_2 [50, 51]. In the last one the values at ambient pressure are: $\partial T_N / \partial \sigma_a = +900$ mK/GPa and $\partial T_N / \partial \sigma_c = -410$ mK/GPa for $T_N = 17$ K. The strain dependence of T_c in URu_2Si_2 illustrates the antagonism between magnetism and superconductivity as the respective variations of T_c and $T_N(\sigma)$ are opposite: $\partial T_c / \partial \sigma_a = -620$ mK/GPa and $\partial T_c / \partial \sigma_c = +430$ mK/GPa for $T_c = 1.2$ K. Huge effects have also been detected in the pressure dependence of T_N in CePd_2Si_2 measured on two crystals with the c axis parallel or perpendicular to the pressure gradient due to the non-hydrostaticity of the pressure cell [49]. Of course, as the superconducting domain is locked at P_c , a large difference appears also in $T_c(P)$. To summarize the broadening is strongly associated to the magnitude of $\partial T_N / \partial P$ and thus the calorimetric anomaly collapses at P_c .

In figure 6 the transition width of the superconducting transition above P_c is shown as function of pressure, and in figure 5 that of the AFM transition below P_c . In this system, due to the competition between AFM and SC order, we rather expect that these respective transition width are related to the strength of the pressure variation of their own critical temperature. What is more, in the 115 series, the main source of heterogeneities may be that internal pressure or strain gradients in the material itself. Thus, local distributions of T_c or T_N may be induced. It is well known that near defects like dislocations or stacking faults, internal strain of the order of 0.1 GPa can occur. Evidences for such an effect are given in the paramagnetic state of CeIrIn_5 at zero pressure as $T_c^p = 1.2$ K is quite different from $T_c^C = 0.4$ K [40].

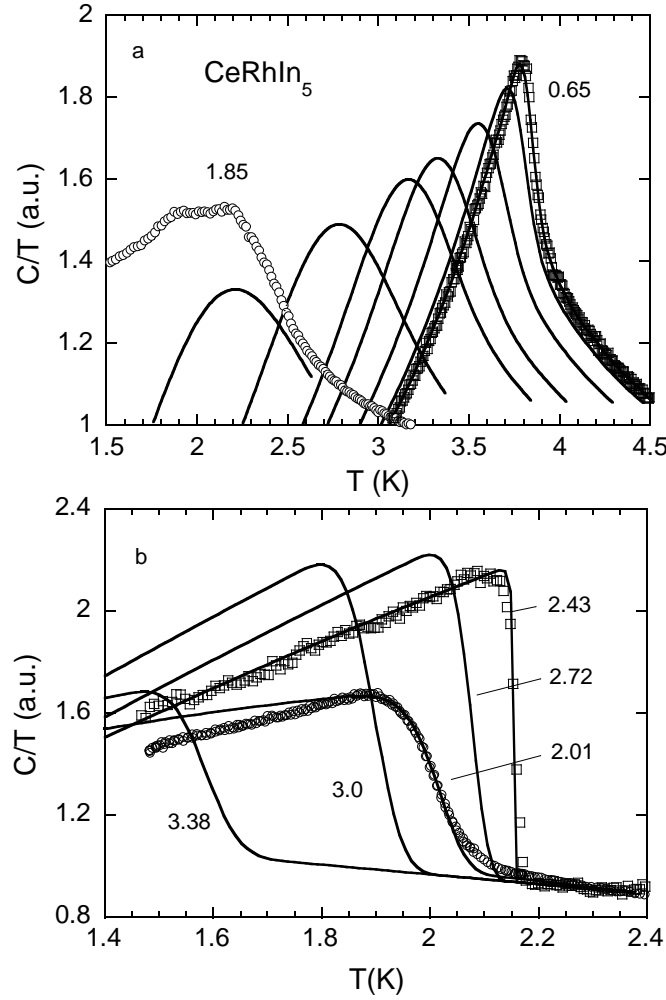


Figure 7. Upper frame a: Modelling of the specific heat of CeRhIn_5 taking into account a pressure distribution of $\Delta P = 0.045$ GPa and the slope of $\partial T_N / \partial p$ for different pressures ($P = 0.65, 0.85, 1.07, 12.7, 13.8, 1.6$ and 1.85 GPa). For comparison the measured specific heat for $P = 0.65$ GPa and 1.85 GPa is plotted. Lower frame b: Effect of the same pressure distribution of $\Delta P = 0.055$ GPa on the superconducting transition.

In that case, the superconducting transition observed by resistivity is clearly due to superconducting filaments. This big mismatch of T_c as measured by resistivity or specific heat seems again directly linked with the difference between $\partial T_c / \partial \sigma_a = 540$ mK/GPa and $\partial T_c / \partial \sigma_c = -840$ mK/GPa [34]. Of course an extra cause of heterogeneity can be induced by the non hydrostaticity of the pressure transmitting medium. However, in our case, the use of argon optimizes the hydrostaticity.

To demonstrate the impact of internal strain or pressure inhomogeneities when $\partial T_N / \partial P$ and $\partial T_c / \partial P$ have a strong pressure dependence, we have calculated the temperature dependence of the specific heat near the antiferromagnetic and the superconducting transition under the assumption of a pressure distribution inside the sample, of width ΔP , which may be caused by the experimental conditions or by

inhomogeneities in the material. For the antiferromagnetic transition (see figure 7a) we suppose that in an hypothetical ideally hydrostatic pressure cell, the shape of the specific heat anomaly would remain unchanged whatever the transition temperature. We have further assumed that at low pressure, the pressure variation of T_N is small and we can take the curve at 0.65 GPa as the ideal curve. Indeed, $\partial T_N / \partial P \approx 0$ for 0.65 GPa, so that pressure gradients should have only minor effects on the shape of C/T . We assume a gaussian pressure distribution inside the sample, so that the form of the specific heat anomaly for an mean average pressure P_0 is given by

$$\left. \frac{C}{T} \right|_{P_0} (T) = \int 1/W(P) \exp \left[-\frac{1}{2} \left(\frac{P - P_0}{\Delta P} \right)^2 \right] \left. \frac{C}{T} \right|_{0.65} \left(\frac{T}{T_N(P)} \right) dP.$$

The weighting factor W includes the normalization of the gaussian distribution, and normalization of $\left. \frac{C}{T} \right|_{0.65} \left(\frac{T}{T_N(P)} \right)$ with respect to entropy balance: $W(P)$ should be proportional to T_N for localized magnetism, or constant for itinerant magnetism. The difference in the resulting curves is found to be insignificant for the pressure distribution involved in this experiment. Calculated specific heat transitions for the experimental pressures P_0 and a pressure distribution of $\Delta P = 0.055$ GPa are shown in figure 7. They have to be compared to the measurements (see figure 1). The broadening in the range where $\partial T_N / \partial P$ is steep, is clearly visible in the calculations and it is in qualitative agreement with the measurements.

A more quantitative comparison between experiment and these calculations has been done for the superconducting transition, with the same pressure distribution $\Delta P = 0.055$ GPa. We have calculated the specific heat near the superconducting transition for $P > 2$ GPa (see figure 7b). The entropy balance imposes that $S_n = S_s$ at T_c for all pressures. We have assumed a power law dependence of $C/T(P) = A(T/T_c)^\alpha$ in the superconducting state [53], adjusting the exponent α (which depends on the relative specific heat jump at T_c) in order to fulfill the entropy balance. So calculation of C/T for a fixed pressure distribution ΔP is controlled by two parameters: $T_c(P)$, which is known from the phase diagram, and the size of the anomaly at the average pressure (which controls α). The comparison with the measurements (see figure 2) shows that the broadening of the transition for pressures below and above the maximum of $T_c(P)$ can be understood with the same fixed pressure distribution.

To summarize, a fixed gaussian pressure distribution of about 0.055 GPa can explain the observed broadening of the antiferromagnetic and the superconducting transitions, as a result of the pressure dependence of T_N and T_c . As regard the origin of this pressure distribution, 0.04 GPa is really the upper limit expected for inhomogeneities inside a pressure cell filled with argon. More reasonably, these inhomogeneities could be due to internal strain and defects in combination with the anisotropic elastic properties of the material [54].

3.4. On the possibility of gapless nature of superconductivity: material effects or novel phase ?

The question of a gapless SC state below P_c started with recent NQR results [21]: just above P_c , the nuclear relaxation time follows the usual behavior of an unconventional SC state with line nodes: below T_c , $(T_1T)^{-1}$ has a nice T^2 dependence. This contrasts with the situation below P_c . For example at 1.6 GPa, below T_c^x , $(T_1T)^{-1}$ reaches rapidly at low temperatures ($T \ll T_N$) a value corresponding to the normal phase [21]. According to Fisher *et al.* [16], the specific heat coefficient γ increases by a factor 3 to 4 from 0 to 1.6 GPa. This increase of the effective mass leads to an increase of $(T_1T)^{-1}$ by one order of magnitude, as observed in the experiment.

We have stressed that our measurements and analysis do not support an intrinsic AFM+SC state between P_{S-} and P_c . However, a gapless state in this pressure region could be possible without any additional line in the phase diagram (a continuous evolution of the gap amplitude collapsing when on approaching P_c from the high pressure region would not necessarily induce symmetry changes). This gapless state cannot be due to impurity scattering, as the criterion for clean limit are satisfied as well below and above P_c : the sample investigated in our measurement has a residual resistivity ratio of almost 200 which shows that it is very clean.

The possibility of the realization of p -wave spin singlet superconductivity, whose gap function is odd in frequency and momentum, was very recently discussed by Fuseya *et al.*[42]. They showed that near a quantum critical point where strong retardation effects are possible, this p -wave state is more likely than the d -wave state which is expected to be realized away from the critical point in the antiferromagnetic as well as in the paramagnetic regime. A quantum critical point is not observed in our experiment, and a gapless region is also not observed above P_c [16]. Nevertheless, this difference might arise from the first order nature of the AFM \rightarrow SC transition. The NQR results were interpreted with a heuristic view in favour of this new class of superconducting phase below P_c which differs from the usual d wave pairing [21]. Basically, the bare experimental features are similar to those observed here: T_c^p , the superconducting onset chosen in resistivity is higher than T_c^x where diamagnetic shielding is observed. T_c^x appears to coincide with the temperature where tiny features appear in the temperature variation of $(T_1T)^{-1}$ of the inverse product of the nuclear relaxation time T_1 by temperature.

From our point of view, the difficulty with this scenario is both quantitative: it is not expected that T_c could rise up to T_N (at P_c), and qualitative: switching from a gapless p -wave state below P_c to a gaped d -wave state above P_c would involve a symmetry change and thus transform the tricritical point at P_c to a tetracritical point. We would rather interpret the "gapless" nature of superconductivity observed by NQR as related to the heterogeneities observed in the magnetic transition. However, it is obvious that the debate remains. An important issue is to discuss more deeply the discrepancy between neutron diffraction and NQR measurements in the AFM phase.

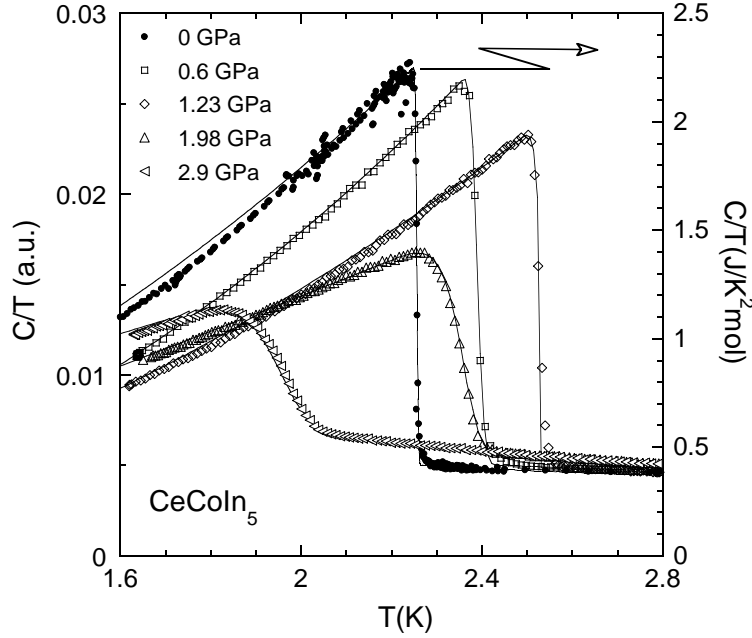


Figure 8. Specific heat of $CeCoIn_5$ under high pressure for different pressures. The ac signal is corrected by a constant background of about 40% of the measured specific heat in the normal state and it is assumed to be linear in temperature and independent of pressure. For comparison, C/T determined by a quantitative measurement is shown ($P = 0$, right scale). Lines are calculations of the specific heat under the assumption of a pressure distribution ΔP which increases linearly under pressure from $\Delta P = 0.015$ for $P = 0$ up to $\Delta P = 0.15$ for $P = 2.9$ GPa.

4. Superconductivity in $CeCoIn_5$ under high pressure

The specific heat under high pressure of $CeCoIn_5$ is shown in figure 8. Up to 1.5 GPa, the anomaly under high pressures is almost as sharp as at ambient pressure, whereas at higher pressures the anomaly start to get broader. The phase diagram obtained from specific heat and ac susceptibility measurements is shown in figure 9. With increasing pressure T_c is increasing with an initial rate of 0.6 K/GPa up to 1.6 GPa, for higher pressure it decreases with a rate of 0.3 K/GPa which is slower than the diminutions of T_c in $CeRhIn_5$. The very large jump at ambient pressure in the specific heat $\Delta C/C(T_c) = 4.5$, which is the largest found in heavy fermion superconductors, was first interpreted as a hint for strong coupling superconductivity in $CeCoIn_5$ [26, 32]. The pressure dependence of the the jump of the specific heat at T_c is shown in figure 10. The height of the jump obtained by Sparn *et al.* was used to determine the background signal for the ac calorimetry and to normalize the jump obtained by ac calorimetry. The background is of about 40% of the measured ac signal in the normal state and it is assumed to be linear in temperature and independent of pressure. By increasing pressure the large jump in the specific heat decreases linearly to $\Delta C/C(T_c) = 1$ at 3 GPa. The reduction of the jump with pressure is clearly an indication of the reduction of the effective mass m^* with increasing pressure. Neglecting strong coupling effects, the jump

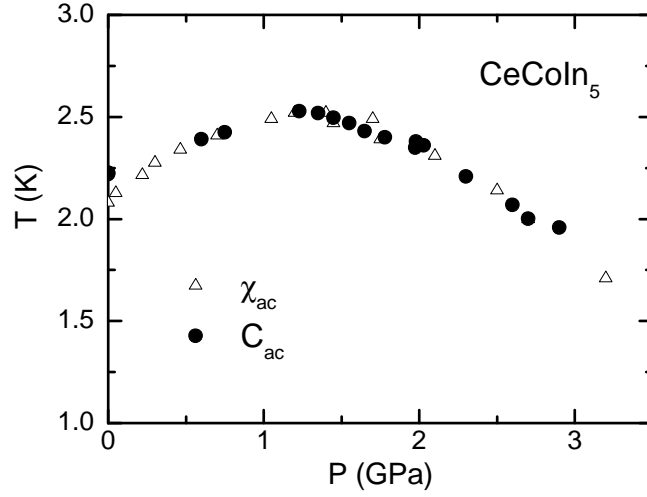


Figure 9. Pressure-temperature phase diagram of $CeCoIn_5$ obtained by high pressure ac calorimetry (●) and ac susceptibility (△).

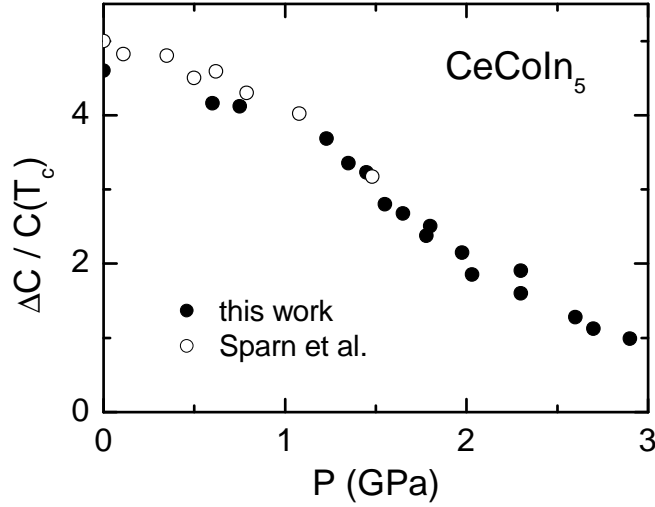


Figure 10. Pressure dependence of the jump of the specific heat at T_c in $CeCoIn_5$. (○) are taken from reference [32] and are used to normalize the jump in the ac calorimetry.

of the specific heat normalized to the effective mass $\Delta C/m^*T_c \propto \text{const.}$ must be fulfilled. However, the weakness of strong coupling is justified by the temperature variation of the upper critical field of $CeCoIn_5$, which can be expressed in a weak coupling model with strong Pauli limitation. The large jump at ambient pressure is due to the fact that superconductivity sets in when the heavy fermion state is not yet formed and the effective mass is still increasing to lower temperatures. Measurements of the specific heat in field at 5 T parallel to c axis show that C/T is increasing to lowest temperatures [9, 52]. The increase of C/T is a strong indication that $CeCoIn_5$ at ambient pressure is close to a magnetic instability and the system can be driven through a quantum critical point by applying a magnetic field higher than the upper critical field. By contrast, at

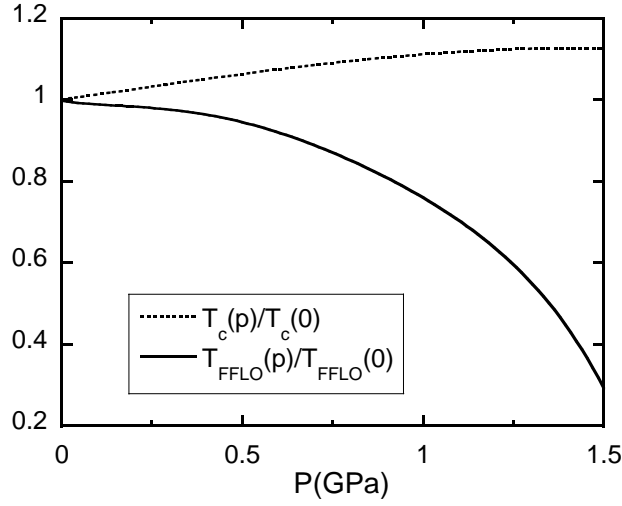


Figure 11. Relative evolution of $T_c(p)$ and $T_{FFLO}(p)$ as deduced from our measurements of $T_c(P)$ and of the Sommerfeld specific heat coefficient. Contrary to naive expectations from the rapid drop of $m^*(P)$, T_{FFLO} is predicted to have only a weak initial pressure variation.

3 GPa superconductivity sets in when the heavy masses are formed and $CeCoIn_5$ behaves as a usual heavy fermion system. The decrease of the effective mass with pressure has been seen directly by de Haas-van Alphen experiments under high pressure [33].

To estimate the influence of pressure inhomogeneities on the superconducting transition in $CeCoIn_5$ we calculated the specific heat in the same manner than for $CeRhIn_5$ (see above). However, in addition the pressure dependence of the effective mass m^* has to be taken into account. The lines in figure 8 are the results of the calculations. Contrasting with $CeRhIn_5$, for $CeCoIn_5$ the pressure distribution increases linearly from $\Delta P = 0.015$ GPa at ambient pressure to $\Delta P = 0.15$ at 2.9 GPa. We can exclude that this increase of inhomogeneity is due to bare pressure gradients. But it could arise from the material itself. As pointed out above, uniaxial stress applied in different crystallographic directions may result in opposite effects on T_c , $\partial T_c / \partial \sigma_a > 0$ and $\partial T_c / \partial \sigma_c < 0$. A stress distribution proportional to the pressure would be the most likely source of this linear increase of ΔP . The effect of "pressure" inhomogeneities is expected to be more important in $CeCoIn_5$ than in $CeRhIn_5$, as the anisotropy of the elastic constants of this compound is the largest of the Ce 115 compounds [55].

Recently the so-called Fulde, Ferrel, Larkin, Ovchinnikov (FFLO) phase has been found in $CeCoIn_5$ below $T_{FFLO} < T_c$ close to the upper critical field $H_{c2}(0)$ for the magnetic field H applied in the basal plane [56, 57, 58, 59, 60]. The key point is that the paramagnetic limit $H_{c2}^p = 1.8T_c$ in Tesla assuming $g = 2$ for the conduction electrons governs the behaviour of the upper critical field at very low temperatures since the orbital limit $H_{c2}^{orb}(0) \approx (m^*T_c)^2$ is far higher than $H_{c2}^p(0)$. Nevertheless, the balance between the orbital and paramagnetic limit is expected to change under pressure, due to the variation of T_c (which controls H_{c2}^p) and of m^* , which controls, together with T_c ,

the H_{c2}^{orb} . In fact, both $T_c(P)$ and $m^*(P)$ are known from our experiment, so we could estimate what should be the relative variation of T_{FFLO} under pressure in a classical calculation of H_{c2} including the FFLO state (see for example reference [61]). It is reported on figure 11. From the strong decrease of the effective mass under pressure, we would have expected a drastic decrease of T_{FFLO} under pressure: this is not the case, due to the initial increase of T_c which compensates the drop of m^* with P . One can predict that T_{FFLO} will start to decrease significantly only near 1.5 GPa, i.e. when T_c reaches its maximum, despite the fact that at this pressure, m^* has decreased by a factor of 2. Of course, this prediction is valid only in a classical scheme: it might be different if for example the interaction itself change with the magnetic field since the FFLO state appears for magnetic fields just above the field H_M where pseudo-metamagnetism may occur [60, 62].

5. Conclusion

We studied the specific heat of $CeRhIn_5$ and $CeCoIn_5$ under high pressure by ac calorimetry and ac susceptibility up to 3.5 GPa. In $CeRhIn_5$ a first order transition from antiferromagnetic order below $P_c = 1.95$ GPa to a superconducting ground state for $P > 2$ GPa has been observed. Below P_c superconductivity and antiferromagnetism coexist. However, in this regime no superconducting specific heat anomaly has been observed which points to an inhomogeneous appearance of superconductivity in this pressure range. Above P_c the very sharp superconducting specific heat anomaly is due to homogenous bulk superconductivity.

The large jump of the specific heat in $CeCoIn_5$ at the superconducting transition is reduced linearly with increasing pressure. This is a clear indication for the decrease of the effective mass with pressure and the system is tuned away from its magnetic instability. At high pressure, $CeCoIn_5$ behaves like a usual heavy fermion superconductor.

Acknowledgments

This work has been supported by the IPMC Grenoble. We thank K. Miyake for fruitful discussions.

- [1] Steglich F, Aarts J, Bredl C-D, Lieke W, Meschede D, Franz W and Schäfer H 1979 *Phys. Rev. Lett.* **43** 1892
- [2] Jaccard D, Behnia K and Sierro J 1992 *Phys. Lett. A* **163** 475
- [3] Movshovich R, Graf T, Mandrus D, Thompson J D, Smith J L and Fisk Z 1996 *Phys. Rev. B* **53** 8241
- [4] Mathur N D, Grosche F M, Julian S R, Walker I R, Freye D M, Haselwimmer R K W and Lonzarich G G 1998 *Nature* **394** 39
- [5] Holmes A T, Jaccard D and Miyake K 2004 *Phys. Rev. B* **69** 024508
- [6] Yuan H Q, Grosche F M, Deppe M, Geibel C, Sparn G and Steglich F 2003 *Science* **302** 2104

- [7] Hegger H, Petrovic C, Moshopoulou E G, Hundley M F, Sarrao J L, Fisk Z and Thompson J D 2000 *Phys. Rev. Lett.* **84** 4986
- [8] Petrovic C, Movshovich R, Jaime M, Paglusio P G, Hundley M F, Sarrao J L, Fisk Z and Thompson J D 2001 *Europhys. Lett.* **53** 354
- [9] Petrovic C, Paglusio P G, Hundley M F, Movshovich R, Sarrao J L, Thompson J D, Fisk Z and Monthoux P 2001 *J. Phys.: Condens. Matter* **13** L337
- [10] Knebel G, Braithwaite D, Canfield P C, Lapertot G and Flouquet J 2001 *Phys. Rev. B* **65** 044425
- [11] Monthoux P and Lonzarich G G 2001 *Phys. Rev. B* **63** 054529
- [12] Moriya T and Ueda K 2003 *Rep. Prog. Phys* **66** 1299
- [13] Fukazawa H and Yamada K 2003 *J. Phys. Soc. Jpn.* **72** 2449
- [14] Shishido H, Settai R, Aoki D, Ikeda S, Nakawaki H, Nakamura N, Iizuka T, Inada Y, Sugiyama K, Takeuchi T, Kindo K, Kobayashi T C, Haga Y, Harima H, Aoki Y, Namiki T, Sato H, Onuki Y 2002 *J. Phys. Soc. Jpn.* **71** 162
- [15] Muramatsu T, Tateiwa N, Kobayashi T C, Shimizu K, Amaya K, Aoki D, Shishido H, Haga Y and Onuki Y 2001 *J. Phys. Soc. Jpn.* **70** 3362
- [16] Fisher R A, Bouquet F, Phillips N E, Hundley M F, Paglusio P G, Sarrao J L, Fisk Z and Thompson J D 2002 *Phys. Rev. B* **65** 224509
- [17] Kohori Y, Yamato Y, Iwamoto Y and Kohara T 2000 *Eu. Phys. J. B* **18** 601
- [18] Mito T, Kawasaki S, Zheng G -q, Kawasaki Y, Ishida K, Kitaoka Y, Aoki D, Haga Y and Onuki Y 2001 *Phys. Rev. B* **63** 220507
- [19] Kawasaki S, Mito T, Zheng G -q, Thessieu C, Kawasaki Y, Ishida K, Kitaoka Y, Muramatsu T, Kobayashi T C, Aoki D, Araki S, Haga Y, Settai R and Onuki Y 2001 *Phys. Rev. B* **65** 020504(R)
- [20] Mito T, Kawasaki S, Kawasaki Y, Zheng G -q, Kitaoka Y, Aoki D, Haga Y and Onuki Y 2003 *Phys. Rev. Lett.* **90** 077004
- [21] Kawasaki S, Mito T, Kawasaki Y, Zheng G -q, Kitaoka Y, Aoki D, Haga Y and Onuki Y 2001 *Phys. Rev. Lett.* **91** 137001
- [22] Bao W, Pagliuso P G, Sarrao J L, Thompson J D, Fisk Z, Lynn J W and Erwin R W 2000 *Phys. Rev. B* **62** R14621; Erratum: 2001 *ibid.* **63** 219901(E)
- [23] Bao W, Trevino S F, Lynn J W, Pagliuso P G, Sarrao J L, Thompson J D and Fisk Z 2002 *Appl. Phys. A* **74** 557
- [24] Majumdar S, Balakrishnan G, Lees M R, McK Paul D and McIntyre 2002 *Phys. Rev. B* **66** 212502
- [25] Llobet A, Gardner J S, Moshopoulou E G, Mignot J-M, Nicklas M, Bao W, Moreno N O, Pagliuso P G, Goncharenko I N, Sarrao J L and Thompson J D 2004 *Phys. Rev. B* **69** 024403
- [26] Movshovich R, Jaime M, Thompson J D, Petrovic C, Fisk Z, Pagliuso P G and Sarrao J L 2001 *Phys. Rev. Lett.* **86** 5152
- [27] Izawa K, Yamagushi H, Matsuda Y, Shishido H, Settai R and Onuki Y 2001 *Phys. Rev. Lett.* **87** 057002
- [28] Ormeno J R, Sibley A, Gough C E, Sebastian S and Fisher I R 2002 *Phys. Rev. Lett.* **88** 047005
- [29] Aoki H, Sakakibara T, Shishido H, Shishido H, Settai R, Onuki Y, Miranović P and Machida K 2003 *J. Phys.: Condens. Matter* **16** L13
- [30] Nicklas M, Borth R, Lengyel E, Pagliuso P G, Sarrao J L, Sidorov V A, Sparn G, Steglich F and Thompson J D 2001 *J. Phys.: Condens. Matter* **13** L905
- [31] Sidorov V A, Nicklas M, Pagliuso P G, Sarrao J L, Bang Y, Balatsky A V, Thompson J D 2001 *Phys. Rev. Lett.* **89** 157004
- [32] Sparn G, Borth R, Lengyel E, Pagliuso P G, Sarrao J L, Steglich F and Thompson J D 2001 *Frontiers of High Pressure Research II: Application of High Pressure to Low Dimensional Novel Electronic Material* ed Hochheimer H D (Kluwer Academic Publishers, Netherlands)
- [33] Shishido H, Ueda T, Hashimoto S, Kubo T, Settai R, Harima H and Onuki Y 2003 *J. Phys.: Condens. Matter* **15** L499
- [34] Oeschler N, Gegenwart P, Lang M, Movshovich R, Sarrao J L, Thompson J D and Steglich F 2003

- Phys. Rev. Lett.* **91** 076402
- [35] Sullivan P F and Seidel G 1968 *Phys. Rev.* **173** 679
 - [36] Demuer A, Marcenat C, Thomasson J, Calemczuk R, Salce B, Lejay P, Braithwaite D and Flouquet J 2000 *J. Low Temp. Phys.* **120** 245
 - [37] Wilhelm H and Jaccard D 2002 *J. Phys.: Condens. Matter* **14** 10683
 - [38] Salce B, Thomasson J, Demuer A, Blanchard J J, Martinod J M, Devoille L and Guillaume A 2000 *Rev. Sci. Instrum.* **71** 2461
 - [39] Cornelius A L, Arko A J, Sarrao J L, Hundley M F and Fisk Z 2000 *Phys. Rev. B* **62** 14181
 - [40] Bianchi A, Movshovich R, Jaime M, Thompson J D, Pagliuso P G and Sarrao J L 2001 *Phys. Rev. B* **64** 220504(R)
 - [41] Kawasaki S, Mito T, Kawasaki Y, Kotegawa H, Zheng G-q, Kitaoka Y, Shishido H, Araki S, Settai R and Onuki Y 2004 *J. Phys. Soc. Jpn.* **73** 1647
 - [42] Fuseya Y, Kohno H and Miyake K 2003 *J. Phys. Soc. Japan* **72** 2914
 - [43] Thomasson J *private communication*
 - [44] Demuer A, Sheikin I, Braithwaite D, Fåk B, Huxley A, Raymond S and Flouquet J 2001 *J. Magn. Magn. Mater.* **226 - 230** 17
 - [45] Haga Y *et al.* unpublished
 - [46] Zülicke U and Millis A J 1995 *Phys. Rev. B* **51** 8996
 - [47] Dotsenko V S 1995 *Phys. Usp.* **38** 347
 - [48] van Dijk N H, Fåk B, Charvolin T, Lejay P and Mignot J M 2000 *Phys. Rev. B* **61** 8922
 - [49] Demuer A, Holmes A T and Jaccard D 2002 *J. Phys.: Condens. Matter* **14** L529
 - [50] de Visser A, Kayzel F E, Menovsky A A, Franse J J M, van den Berg J and Nieuwenhuys G J 1986 *Phys. Rev. B* **34** 8168
 - [51] van Dijk N H, de Visser A, Franse J J M and Menovsky A A 1995 *Phys. Rev. B* **51** 12665
 - [52] Bianchi A, Movshovich R, Vekhter I, Pagliuso P G and Sarrao J L 2003 *Phys. Rev. Lett.* **91** 257001
 - [53] As we are only interested in the temperature range very close to T_c , the correct form of C/T is not of great importance for the calculation of the broadening of the transition.
 - [54] Kumar R S, Kohlman H, Light B E, Cornelius A L, Raghavan V, Darling T W and Sarrao J L 2004 *Phys. Rev. B* **69** 014515
 - [55] Kumar R S, Cornelius A L and Sarrao J L 2004 cond-mat/02405043
 - [56] Tayama T, Harita A, Sakakibara T, Haga Y, Shishido H, Settai R and Onuki Y 2002 *Phys. Rev. B* **65** 180504
 - [57] Murphy T P, Hall D, Palm E C, Trozer S W, Petrovic C, Fisk Z, Goodrich R G, Pagliuso P G, Sarrao J L and Thompson J D 2002 *Phys. Rev. B* **65** 100514
 - [58] Bianchi A, Movshovich R, Oeschler N, Gegenwart P, Steglich F, Thompson J D, Pagliuso P G and Sarrao J L 2002 *Phys. Rev. Lett.* **89** 137002
 - [59] Bianchi A, Movshovich R, Capan C, Pagliuso P G and Sarrao J L 2003 *Phys. Rev. Lett.* **91** 187004
 - [60] Radovan H A, Fortune N A, Murphy T P, Hannahs S T, Palm E C, Trozer S W and Hall D 2003 *Nature* **425** 51
 - [61] J.P. Brison, N. Keller, A. Verniere, P. Lejay, L. Schmidt, A. Buzdin, J. Flouquet, S.R. Julian and G.G. Lonzarich, *Physica C* 1995 **250** 128
 - [62] Paglione J, Tanatar M A, Hawthorn D G, Boaknin E, Hill R W, Ronning F, Sutherland M, Taillefer L, Petrovic C, and Canfield P C, *Phys. Rev. Lett.* **91** 246405